Combustion Analysis of a Hydrogen DI-Engine using non-invasive optical Methods

Hermann Rottengruber, Martin Schenk, Edgar Berger
BMW Group
Advanced Powertrain Development /
SI Engine Functions and Thermodynamics Dept.

1. Introduction

In the course of the on-going further development of hydrogen engines at BMW, investigations are being carried out on H_2 combustion engines with internal as well as external mixture formation. Based on the findings obtained so far, it has been possible to resolve the conflict between high power output and low emissions, a conflict that is allegedly particularly applicable to hydrogen operation.

Hydrogen is a carbon free fuel, so only NO_x emissions are relevant. NO_x emissions are avoided, a high degree of efficiency is achieved, by utilizing an operating strategy that is adapted to hydrogen operation and involves burning a very lean mixture in the part-load range. At the transition point to higher loads, operation switched to stoichiometric operation from the NO_x formation limit onwards (λ=1/Φ=2.2), thereby facilitating exhaust gas aftertreatment (**diagram 1**).

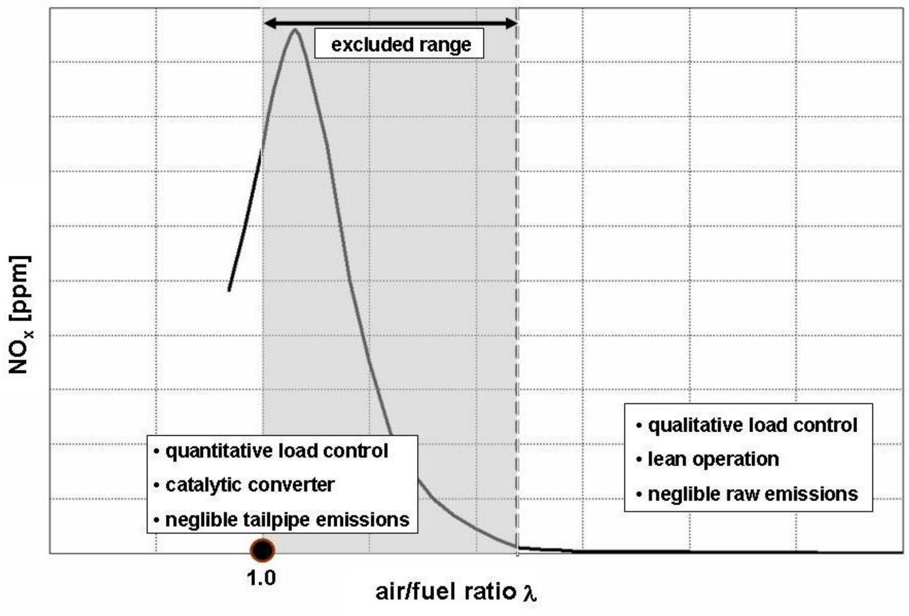

Diagram 1: NO_x operating strategy

By using an adapted charge exchange and injection strategy, it is possible to operate the engine with a homogenous stoichiometric mixture across the entire operating range [1], [2].

By operating at λ=1 it is possible to develop combustion processes with high power densities and at the same time keep exhaust emissions extremely low [1], [3], [4].

External mixture formation brings disadvantages in terms of cylinder charging, since gaseous hydrogen displaces part of the intake air. Even at λ=1, the power output penalty resulting from this cylinder charging disadvantage alone is around 20%, when compared with a spark-ignition engine operating on gasoline. In other words, a naturally-aspirated hydrogen engine with external mixture formation and operating at λ=1 has, with respect to the calorific value of the mixture in the cylinder, a theoretical power output potential that is approx. 84% that of a naturally-aspirated gasoline engine with external mixture formation. This disadvantage can be compensated for either by pressure-charging in combination with external mixture formation or by directly injecting the hydrogen after intake-valve closure.
Hydrogen direct injection, though, requires higher injection pressures. A naturally-aspirated hydrogen engine with internal mixture formation and operation at λ=1 has, with respect to the calorific value of the mixture in the cylinder, a power output potential that is approximately 120% that of a naturally-aspirated gasoline engine with external mixture formation (**diagram 2**).

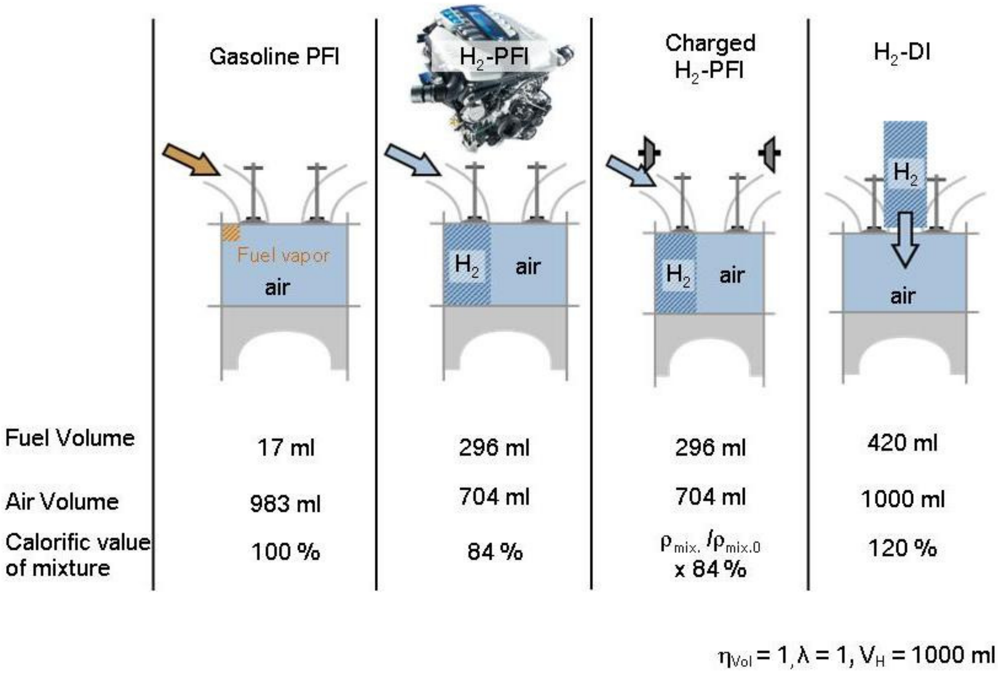

Diagram 2: Calorific values of mixtures for different engine concepts

The following shows various methods of optimizing the full-load behavior of the DI hydrogen combustion process. The power output and efficiency potential is discussed and verified using optical measuring procedures and 3D flow simulations (CFD-simulations).

2. Experimental Setup

The tests were carried out on a single-cylinder engine which is particularly suitable for an accurate investigation of the thermodynamic engine process.

The base engine is in the form of a RICARDO Hydra MK4® single-cylinder research engine. From a design and geometry point of view, the components were based on the current series of BMW 6-cylinder engines. The exact specifications of the test engine can be found in the following table.

displacement	$V_H = 0.5\ dm^3$
stroke	S = 90 mm
bore	d = 84 mm
compression ratio	$\varepsilon = 12:1$
Hydrogen injection pressure	40 – 150 bar
engine speed range	n = 700 to 4000 rpm
mass balancing	normal balancing
max. combustion chamber pressure	120 bar

Table 1: Research engine technical data

For optical investigations of the mixture formation, an optically-accessible single-cylinder engine with the same geometric configuration was used.

As part of the investigations presented here, two cylinder head variants were analyzed (**diagram 3**). In both cases, they were 4-valve cylinder heads with two overhead camshafts. Continuously variable valve timing within the 80 – 160 °CA valve spread limits was made possible by using the VANOS system.
The main differences between the two variants were in the position of the hydrogen injection nozzle. On variant 1 (central location), the injector is located in the center between the valves. In variant 2 (side or lateral location), the injector is positioned below the intake ports which limited design freedom somewhat for the intake port geometry.

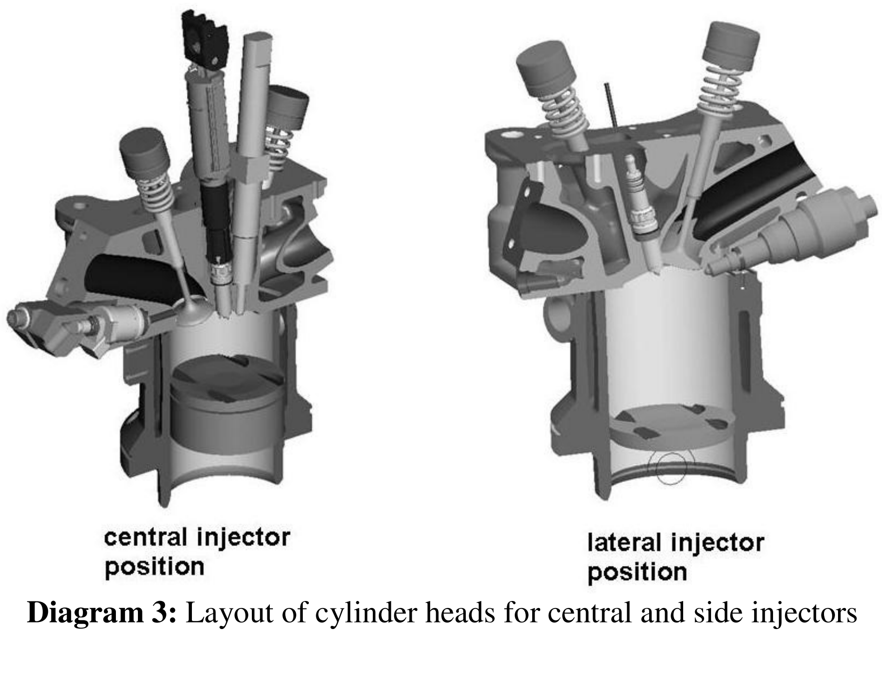

Diagram 3: Layout of cylinder heads for central and side injectors

Injection of hydrogen was performed supercritically at pressures of between 40 and 150 bar during the compression stroke. The injectors used are designed for a rated pressure of 150 bar. Because of the limited flow and restrictions on the dynamics of the electromagnetically-actuated injectors used, sample tests were carried out to identify any potential for reducing the injection pressure.
In addition to the thermodynamic analysis of the hydrogen DI engine process, which requires the recording of integral measurement data such as static temperatures and pressures, and exhaust gas measurements, high and low-pressure indication was also carried out. The pressure indication provided a basis for process analyses and numerical simulations such as one-dimensional flow simulation and thermodynamic loss analysis [1], [4], [12].
The VISIOLution® visualization system from AVL was also employed to provide a more detailed analysis of the fundamental processes of ignition and knock.
Thanks to the use of spark plugs fitted with optical fibers, this system enables flame propagation to be determined without the need to interfere with the design of the engine hardware and the location of any knock centers and auto-ignition events.
The measuring principle used here was the high time-resolution determination of light intensity during combustion using photo diodes. The measuring system, and the physical properties behind it, is dealt with in detail in [5].

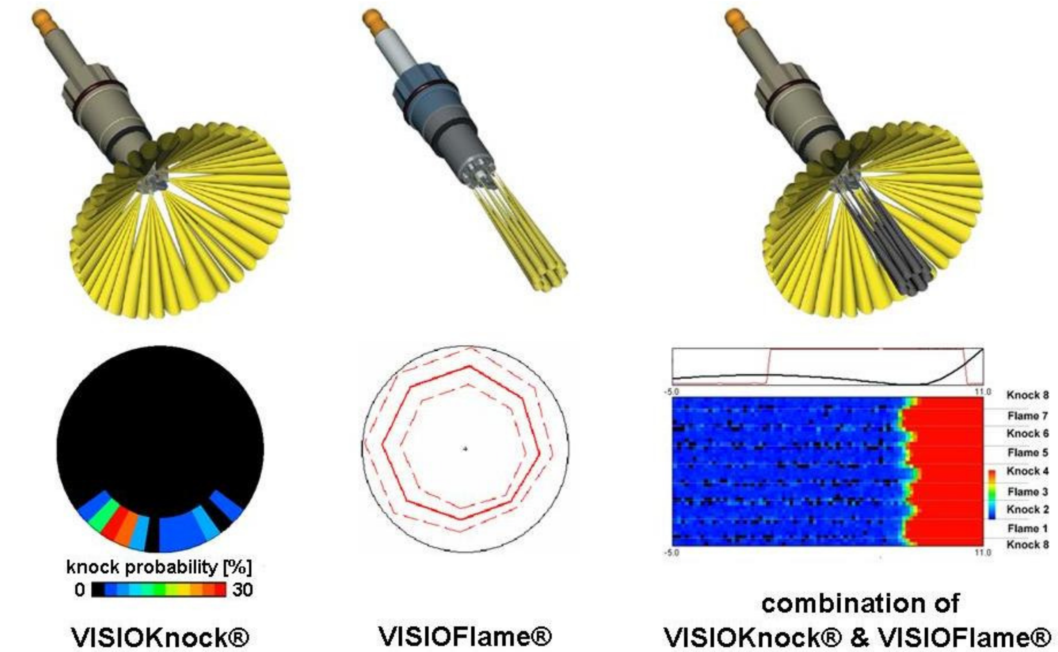

Diagram 4: The different transducer layouts for the AVL VISIOLution® systems

Essentially, a distinction can be made between two different test methods:
The VISIOFlame® system consists of a measuring spark plug with sensors which are directed downwards at the piston (see **diagram 4**). This procedure enables combustion rate and flame kernel propagation to be determined.

The VISIOKnock® spark plug enables knock locations to be determined. The conical sensors are directed outwards and enable statements about combustion anomalies to be made.
A hybrid form of the spark plug (a combination of the two systems, VISIOFlame® and VISIOKnock®) also enables statements to be made about auto-ignition centers. In this set-up, some of the transducers are pointing toward the piston crown, whilst the other sensors are used to record the processes happening at the outer edge of the combustion chamber (**diagram 4**). This configuration enables combustion anomalies to be analyzed with regard to cause and location of occurrence.

3. Full-Load Engine Test and Simulation Results

Power Output Potential

In an analysis of a hydrogen engine with external mixture formation, a maximum engine load of 9 bar mean indicated pressure p_{mi} is achieved (**diagram 5**).
This corresponds to approx. 65-70% of the load of a comparable spark-ignition gasoline-fueled engine. As mentioned in Section 1, this is due to the lower calorific value of the cylinder charge.

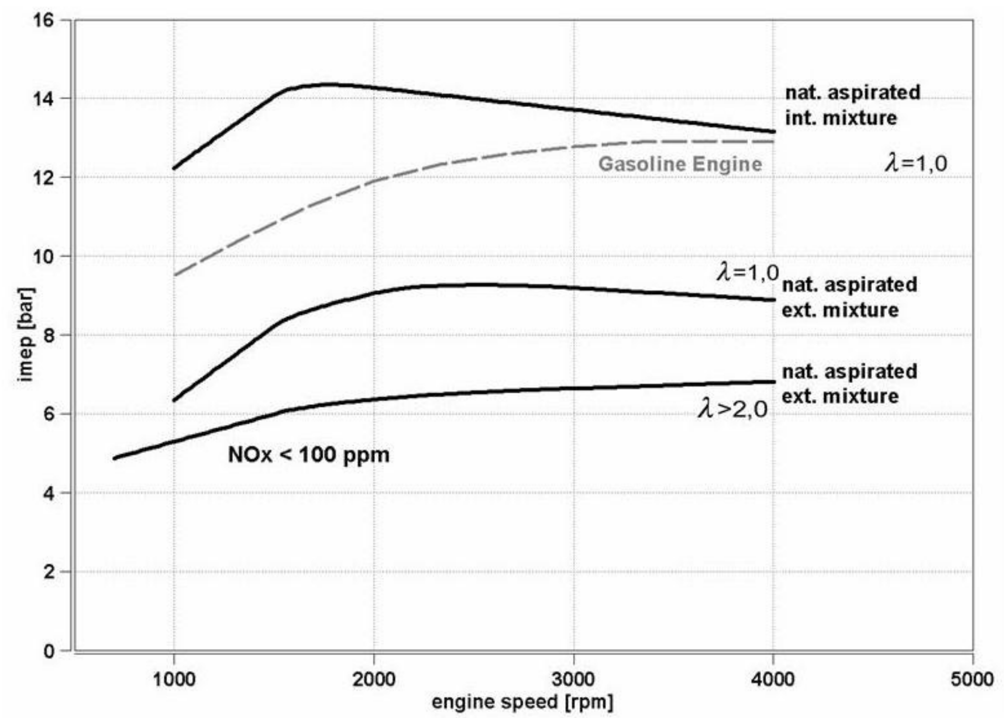

Diagram 5: Full load potential of hydrogen engine concepts

As can also be seen from **diagram 5,** in this regard, a hydrogen engine with internal mixture formation offers considerably greater potential. Based on the engine concept dealt with here, maximum engine loads which are more than 20% above those of a comparable gasoline engine, are achieved [2].
In addition, a substantial increase appears possible at 2000 rpm and an air/fuel ratio of λ=0.9, where a mean indicated pressure of 15 bar is observed.

The reason for this better utilization of potential is the higher calorific value of the mixture. In addition, stoichiometric hydrogen/air mixtures in particular demonstrate better combustion properties than gasoline/air mixtures.

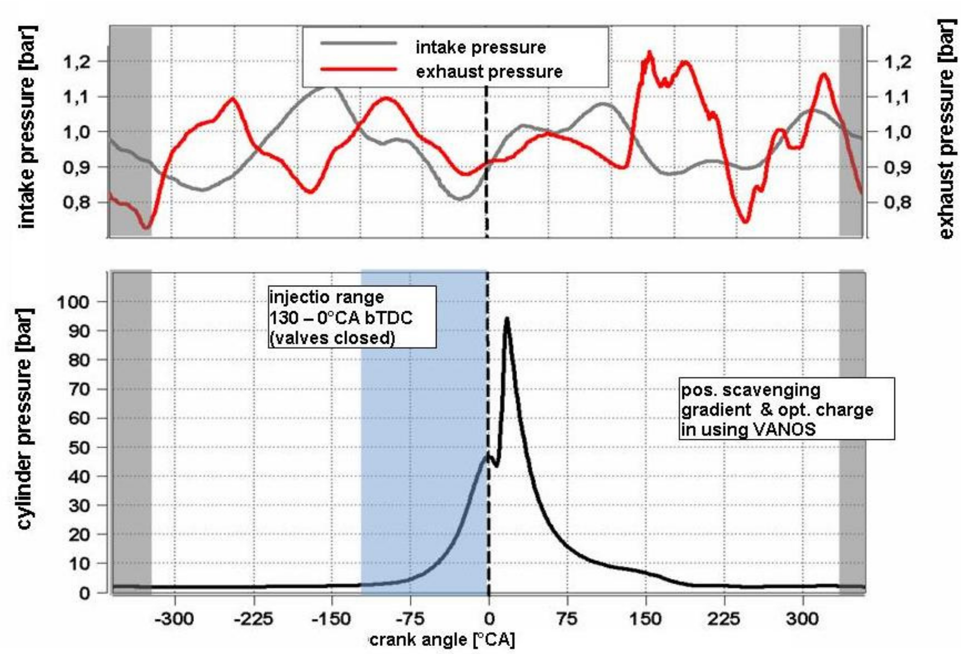

Diagram 6: Injection strategy for H_2 DI operation

The injection strategy also has a considerable influence on the work process in hydrogen direct injection (**diagram 6**). Pre-mixing during compression proved to be a productive strategy. When combined with optimized combustion chamber flushing – achieved thanks to the variability offered by the VANOS system – it can be demonstrated that efficient, reliable engine operation can be achieved through specially targeted injection during the compression stroke.

Injection during the compression stroke brings together several advantages:

- The homogenization of air and hydrogen is improved, which has a positive influence on combustion and the thermodynamic process;
- The required injection pressure can be kept low, resulting in an improvement in the overall energy balance and in the vehicle range in use;
- Cycle fluctuations are minimized as ignition sparks are not influenced by the injection.

As is known from the literature [6], [7] and previous investigations [1], [4], the high combustion rates and the more intensive burn behavior of stoichiometric hydrogen/air mixtures have a significant effect on power output and efficiency, particularly at full load.
Investigations into the burn behavior of stoichiometric hydrogen/air mixtures were carried out with the aid of the reaction kinetic software CHEMKIN (**diagram 7**).

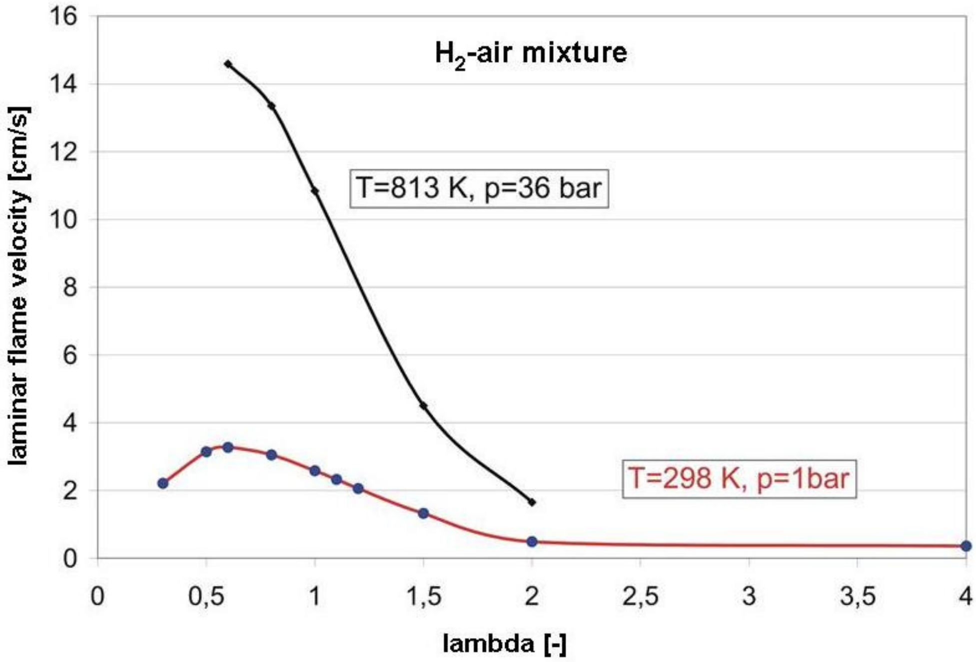

Diagram 7: Reaction kinetic simulation of combustion rate under boundary engine conditions using CHEMKIN

Under the boundary conditions employed, which relate to boundary conditions of the engine process, it was possible to quantify, for this particular application, the tabulated values for standard boundary conditions from the literature.
As can be seen in **diagram 8**, analogous to these results, the combustion curves of an H_2 DI concept at full load (in this case 2000 rpm at the knock limit) differ greatly from those of a spark ignition gasoline engine with comparable power output.
It is noticeable that the moment of ignition for the two hydrogen pressure curves is retarded. This is a result of fast combustion. This setting facilitates a good combustion center, combined with acceptable pressure rise rates.
On the variant with external mixture formation, however, there is a tendency for auto-ignition or premature ignition to occur, as a result of which the useable ignition angle range is limited. In addition, a compression ratio of $\varepsilon=11$ was selected for this engine concept in order to minimize the likelihood of uncontrolled combustion occurring.

By contrast, it was possible to set a compression ratio of $\varepsilon=12$ for the hydrogen DI variant. The shorter time that the hydrogen/air mixture spends in the combustion chamber, the increased turbulence in the combustion chamber as a result of injection during the compression phase and the resulting faster combustion are decisive factors contributing to the drastic reduction in auto-ignition tendency in DI operation. As a result, it is possible to increase the compression ratio to $\varepsilon=12$.

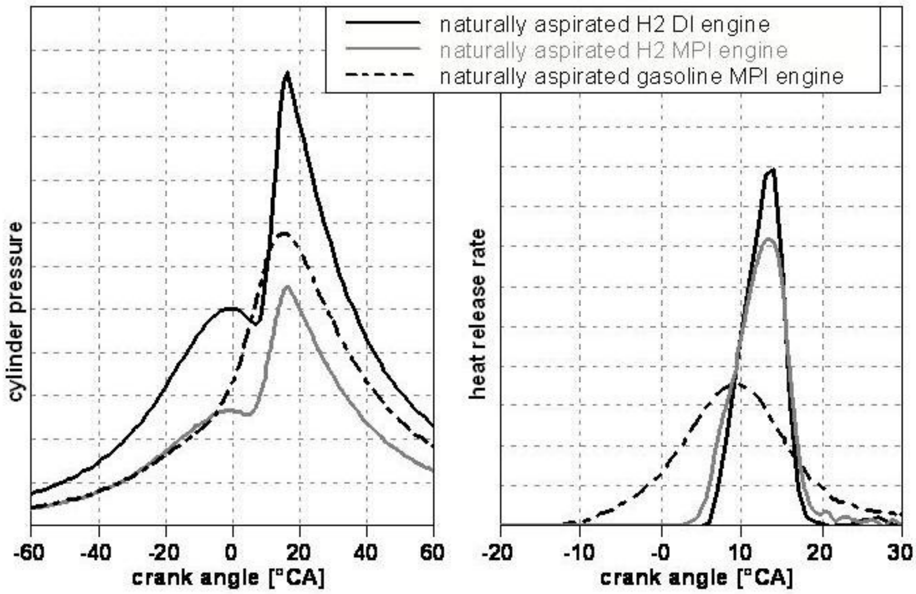

Diagram 8: Comparison of combustion duration of different concepts

This higher compression ratio, compared with the hydrogen MPI variant (ε=11.0) and the gasoline variant (ε=10.2), combined with the increase in pressure as a result of injection, also results in a considerably higher compression end pressure. Furthermore, it is possible to reduce part-load fuel consumption of the hydrogen DI concept compared with that of the hydrogen MPI variant, whilst simultaneously maintaining good full-load volumetric efficiency.

Effect of Injector Position

Because of the high thermal load that the H_2 DI injector is exposed to when positioned centrally, the obvious thing to do is to reduce the thermal load by moving the injector to below the intake valves.

The achievable mean pressure is somewhat higher for the centrally-mounted injector, whilst specific indicated fuel consumption is approximately the same. The reason for this is that the cylinder head with central injection has a slightly higher isentropic flow cross section. The central injector position also has minor advantages in terms of combustion stability. The mean pressure variation coefficient does not fluctuate so greatly, resulting in improved smooth-running performance.

In operation, a virtually identical sensitivity to auto-ignition and combustion anomalies was observed, in other words, the injection and charge exchange parameters could be varied within the same limits.

The investigations carried out on the optical engine in order to correlate CFD simulations, amongst other things, showed very good agreement between measurements and simulations with regard to spray propagation and charge stratification (**diagram 9**).

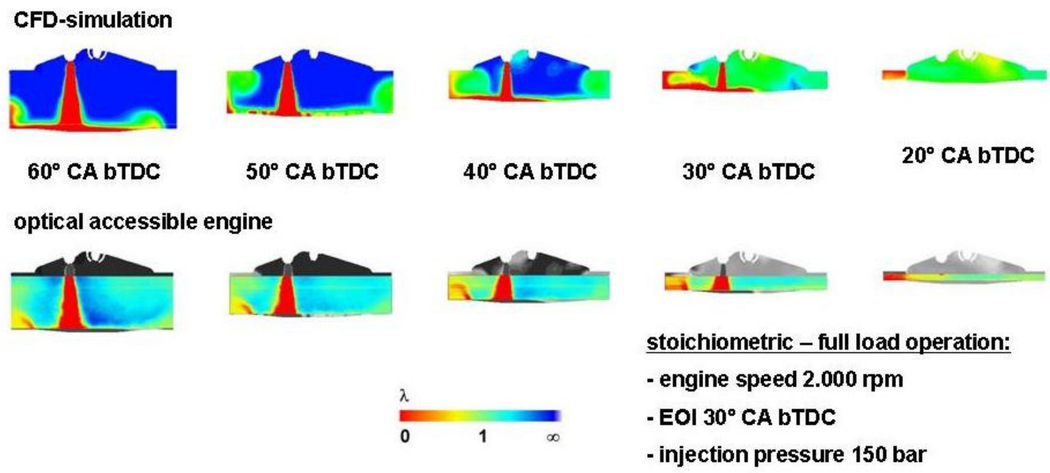

Diagram 9: Comparison of mixture formation on the optical engine with CFD simulation

The areas where moderate hydrogen enrichment occurs in the combustion chamber are identical. Thanks in particular to the cross sensitivities of the tracer used for laser-optical LIF measurement, it is possible to make good quantitative statements about the distribution of the air/fuel ratio and with sufficient accuracy [4], [9].

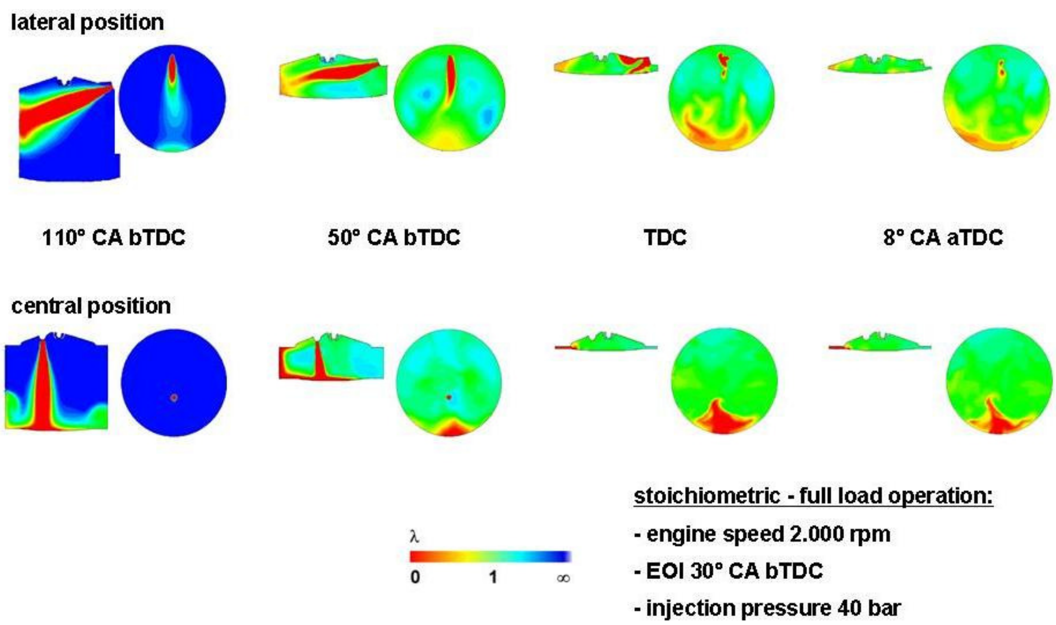

Diagram 10: CFD simulation of the mixture formation for side and central injector positions

An evaluation of the CFD simulation for one full-load operating point at 2000 rpm and an injection pressure of 40 bar (**diagram 10**) clearly reveals very good mixing and only slight deviations from a homogenous λ-distribution throughout the entire combustion chamber.

The same result is also obtained from the standard deviation for the charge density distribution as a function of combustion chamber volume $^*Y_{H2}$ (**diagram 11**).

From the hydrogen mass fraction: $$Y_{H2} = \frac{\rho_{H2}}{\rho}$$

and the standard deviation for density distribution $$^*Y_{H2} = \frac{\int_V \sqrt{\left(\overline{\rho \cdot Y_{H2}} - \rho \cdot Y_{H2}\right)^2}\, dV}{V \cdot \overline{\rho \cdot Y_{H2}}}$$

is derived the measure for homogenization $$^*Y_{H2} = \frac{\int_V \sqrt{\left(\overline{\rho_{H2}} - \rho_{H2}\right)^2}\, dV}{V \cdot \overline{\rho_{H2}}}$$

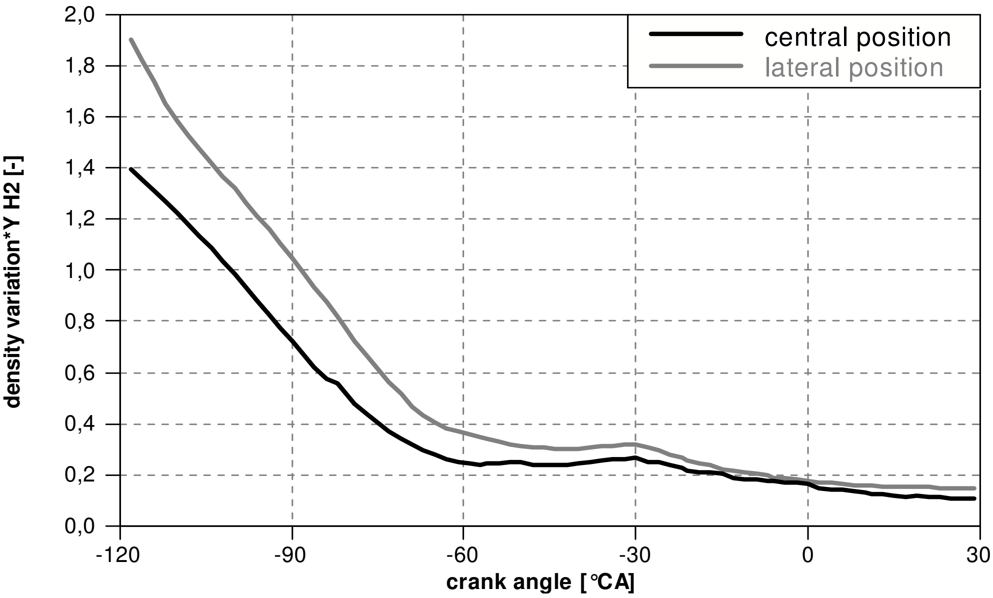

Diagram 11: Density distribution of cylinder charge as a measure for mixture homogenization

For both configurations, the standard deviation for density distribution, which is plotted as a resulting variable from the CFD simulation, converges uniformly from cylinder TDC to a very low level of less than 0.2 units.

Subsequent investigations showed that changes to the injection parameters for the side injector configuration had a considerable influence on combustion. The reason for this is that the hydrogen is injected at an angle across the combustion chamber and over a large distance. As a result of this fact, mixture formation is heavily dependent on injection time, injection pressure and piston position. This dependency can be utilized in order to implement specifically-targeted measures to influence mixture formation, and hence combustion, and to optimize it.

Effect of Injection Pressure

As was shown in the previous chapter, the parameters start of injection and injection duration both have a significant influence on combustion behavior. The injection pressure also has a direct relationship with these variables. When selecting the injection pressure for a hydrogen DI engine concept, however, the following conflicts of aim emerge.

The increase in specific power density makes it necessary to inject the entire quantity of fuel in the period between intake valve closure and ignition timing. A high injection pressure of 150 bar offers the opportunity of varying the start of injection within these limits. An injection pressure limit of $pH_2 \geq 40$ bar is sufficient to guarantee supercritical injection over the entire compression stroke (**diagram 12**).

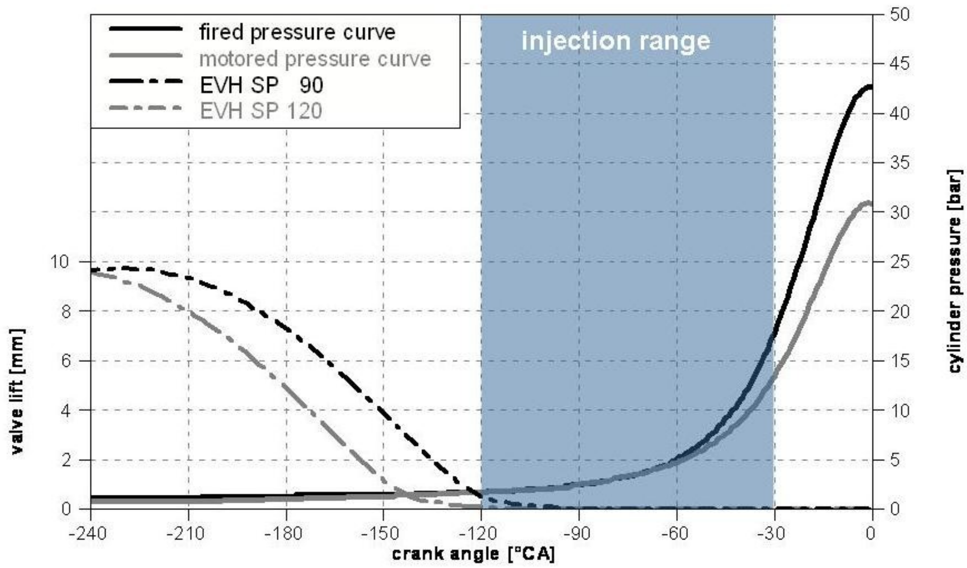

Diagram 12: Configuring the minimum required injection pressure using measured cylinder pressure curves

Reducing the injection pressure makes it easier to provide the required level of pressure on board. By contrast, a very high static flow rate is required so that a sufficient quantity of hydrogen can be supplied, especially at higher engine speeds. In other words, in order to increase the flow rate, the flow-restricting injector cross-section must be enlarged. In the same way, the choice of the start of injection – which is important for charge homogenization and for its effect on pre-ignition tendency - is limited at low injection pressures.

Effect of Injection Timing

The position of injection with respect to the top dead center is adjusted by means of the End of Injection (EOI) parameter.

The adjustment limit for “advancing” this parameter is the closing angle of the intake valve. Injection while the intake valve is open must be avoided in order to prevent the ignitable mixture from flowing back into the intake pipe and air from being displaced

by fuel. The adjustment limit when “retarding” this parameter is the moment of ignition, since injection during combustion has a negative effect on combustion stability. In addition, it was shown in [11] that an injection strategy with specific homogenization during the compression stroke delivers excellent results in engine operation.
As can be seen in **diagram 13**, the cylinder pressure rises as start of injection is advanced resulting in an increase in the useful work of the combustion process. At the same time, the compression work to be done by the piston increases because, unlike gasoline or diesel direct injection, the direct injection of hydrogen into the enclosed combustion chamber results in a reasonable increase in cylinder pressure. Injection causes thermodynamic losses to occur, the amount of which is dependent on start of injection and injection duration, the losses being at the highest when injection is advanced considerably. Consequently, the highest maximum cylinder pressure is achieved when injection is advanced as far as possible (EOI of 90° CA BTDC), but the maximum indicated mean pressure is achieved when EOI is 30° CA BTDC.

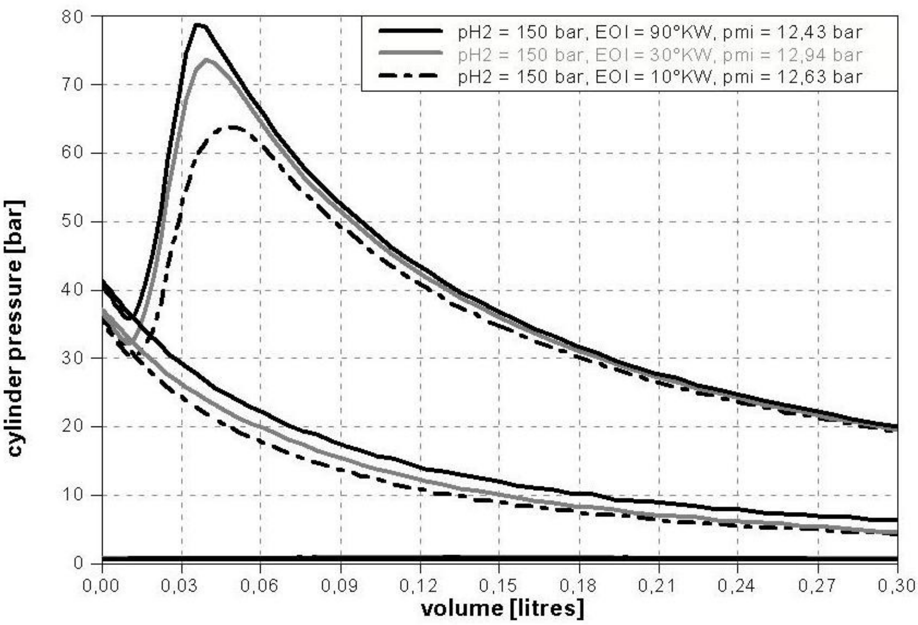

Diagram 13: Influence of end of injection in the p-V diagram at 2000 rpm / full-load

Alongside the additional compression work that has to be done, mixture formation and consequently the combustion rate also have a significant influence. According to [7], [13], [14], the laminar combustion rate of the flame is at its highest in the λ=0.5 range, and drops dramatically from an air/fuel ratio of approx. λ≈1 as the mixture gets increasingly leaner.

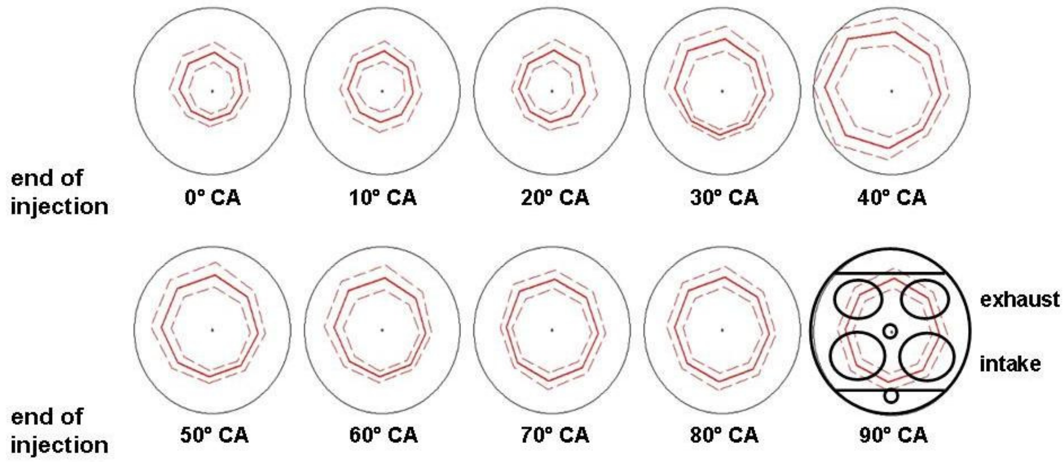

Diagram 14: Flame propagation as a function of end of injection, as calculated with VISIOFlame®

Against this background, the VISIOFlame® results shown in **diagram 14** produce the following findings: when injection timing is retarded, a lean mixture is present at the spark plug, with the result that combustion is slower. Though the introduction of kinetic energy by the injection process has an advantageous effect on combustion behavior, this effect is overcompensated by the incomplete homogenization that occurs when end of injection is very late.

If injection is advanced to 40° CA BTDC, the combustion rate rises significantly, resulting in a locally rich mixture at the spark plug. The shift of the combustion towards the exhaust valves indicates that homogenization of the cylinder charge is still not complete. If injection is advanced further, the combustion rate starts to fall again initially, but then remains more or less constant up to an EOI of 90° CA BTDC. The improved homogenization prevents local leaner or richer mixtures from occurring in the combustion chamber. Uniform combustion propagation also indicates a homogenous mixture.

Thermodynamic loss analysis confirms these interrelationships, which were also observed in the tests on the optical and thermodynamic engine.

The method of loss analysis enables the thermodynamic losses from the combustion process to be quantified. Here, the loss of efficiency caused by the individual losses is calculated using model-based calculations [8], [10], [12]. In addition to the losses which arise because of deviations from the ideal constant-volume process, the injection losses arising as a function of EOI also have an effect on the engine process (**diagram 15**).

As with the thermodynamic test, here too it can be seen that the maximum internal efficiency is achieved with an EOI of 30° CA BTDC. If the injection is advanced more than this, the losses arising from the injection process itself in particular are at their greatest. If injection is retarded, the time remaining for the mixture to homogenize sufficiently is too short. The stratification of the charge and the high turbulence caused by retarded injection result in high wall heat losses which have a negative impact on internal efficiency. Though this effect, which is primarily the result of the high level of turbulence, is partly compensated for by a reduction in the losses from incomplete combustion, this advantage, as is also shown in [15], is not sufficient to achieve an increase in efficiency.

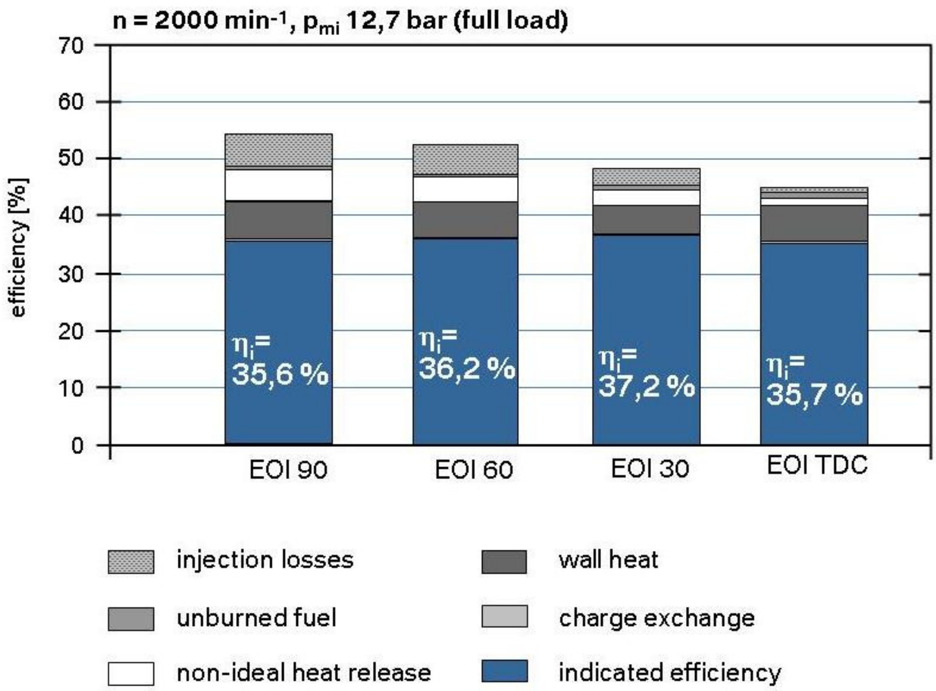

Diagram 15: Thermodynamic losses with varying EOI

Consequently, the observed optimum at an EOI of 30°CA BTDC is a result of the three different mechanisms, namely:

- level of turbulence,
- degree of homogenization and
- thermodynamic losses through injection.

4. Summary

Using the investigations shown here, it has been possible, to demonstrate the considerable potential of a H_2 DI engine concept with regard to power density and efficiency, particularly in the high load range. The combustion engine operated with hydrogen permits levels of power density and power output that are on par with today's gasoline engines.

Results from a comparison, carried out under full load conditions, of two different cylinder head concepts revealed that the engine behavior of both variants was to a large extent similar. The engine concept with a centrally-mounted injector facilitated a slightly higher engine load due to better cylinder charging on account of an intake port which was more favorable to flow. Another result revealed that the cylinder head concept with side-mounted injector demonstrated additional potential for

optimization with regard to H_2 injection parameters. The reason for this is that the hydrogen is injected at an angle through the combustion chamber over a large distance. As a result, the mixture formation is heavily dependent on injection time, injection pressure and piston position. This dependency presents an opportunity for implementing specific measures to influence mixture formation, and thereby combustion. The findings from the thermodynamic test on the single-cylinder engine were verified with the aid of laser-optical investigations and CFD simulations.
Varying the start of injection showed that if injection ends later, losses caused by H_2 injection decrease significantly. At the same time, wall heat losses caused by the increased turbulence during combustion and charge stratification increase. Using the available simulation tools, such as a loss analysis adapted for hydrogen DI operation and 1D and 3D flow simulations, it was possible to obtain important findings for subsequent development stages.

5. Nomenclature and abbreviations

PFI	Port Fuel Injection (external mixture formation)
MPI	Multi Point Injection (external mixture formation)
DI	Direct Injection (internal mixture formation)
VANOS	variable Nockenwellen Steuerung (variable camshaft valve timing)
λ	Air/fuel ratio (equals $1/\Phi$)
Φ	Equivalence ratio, equals $1/\lambda$)
ε	Compression ratio
p_{mi}	Mean indicated pressure
p_{H2}	Hydrogen pressure
b_i	Indicated specific consumption
p	Cylinder pressure at start of compression (at ES)
η_i	Indicated efficiency
VAK	Variation coefficient
n	Engine speed
CA	Crank angle
TDC	Top dead center
BTDC	Before top dead center
ATDC	After top dead center
ES	Intake valve closure point
ZZP	Moment of ignition
EOI	End of Injection
SOI	Start of Injection
t_i	Duration of injection
CFD	Computational Fluid Dynamics, 3D flow simulation
Y	Standard deviation, density distribution in combustion chamber
V_H	Displacement
s	Stroke
d	Bore
H_2	Hydrogen
NO_x	Nitrogen Oxides

6. References

[1] Berckmüller M., Rottengruber H., Eder A., Brehm N., Elsässer G., Müller-Alander G., Schwarz C.: Potentials of a Charged SI-Hydrogen Engine, SAE Paper 2003-01-3210.

[2] Rottengruber H., Berckmüller M.,. Elsässer G., Brehm N., Schwarz C.: A High-Efficient Combustion Concept for Direct Injection Hydrogen Internal Combustion Engines, World Hydrogen Energy Conference XV, Yokohama, Japan 2004

[3] Göschel, B.: The hydrogen combustion engine: propulsion system for the BMW of the future, 24th International Vienna Engine Symposium, Vienna, 2003

[4] Rottengruber H., Berckmüller M., Elsässer G., Brehm N., Schwarz C.: Direct-Injection Hydrogen SI-Engine – Operation Strategy and Power Density Potentials. SAE Paper 2004-01-2927

[5] Winklhofer E., Beidl C., Philipp H., Piock W.: Optical combustion diagnostics with easy to use sensor systems, Motortechnische Zeitschrift MTZ 62 (9); 2001

[6] Zinner K.: Experiences with high-compression gas engines, Motortechnische Zeitschrift MTZ 9 (4 & 5/1948)

[7] Göschel, B.: Alternative drives, script of a lecture, Graz Technical University, 2004

[8] Berckmüller M., Rottengruber H., Eder A., Brehm N., Elsässer G., Müller-Alander G., Schwarz C.: The hydrogen combustion engine with high specific power output – a realistic alternative to gasoline and diesel engines. Fuels and drives of the future – synergies for a sustainable future?, 20th international VDI/VW joint conference, 2003, Wolfsburg

[9] Blotevogel T., Egermann J., Goldlücke J., Leipertz A., Hartmann M., Schenk M., Berckmüller M.: Developing planar laser-induced fluorescence for the investigation of the mixture formation process in hydrogen engines, SAE-Paper 2004-01-1408

[10] Witt, A.: Analysis of thermodynamic losses from a spark-ignition engine under boundary variable valve timing conditions, Dissertation, Graz Technical University, 1999

[11] Rottengruber H., Berckmüller M., Elsässer G., Brehm N., Schwarz C.: Direct injection hydrogen engine – operating strategies and potential, gas vehicles – the right answer to the CO2 challenges of the future?, Haus der Technik/IAV joint conference, Berlin 2004

[12] Eichlseder H., Pischinger R., Wallner T., Wimmer A., Pirker G., Ringler J.: Thermodynamic analysis of spark-ignition engine combustion processes and fuels and their potential, Proceedings from the symposium on development trends in spark-ignition engines, Esslingen, Germany, 2002

[13] Drell I., Belles F.: Survey of Hydrogen Combustion Properties; NACA-Report No. 1383; 1958, URL: http://naca.larc.nasa.gov/reports/1958/naca-report-1383/naca-report-1383.pdf , 18.5.2005

[14] Winter C.-J, Nitsch J. (Hrsg.): Hydrogen as an Energy Carrier, Springer-Verlag Berlin/Heidelberg, 1986, ISBN 0-387-18896-7

[15] Wimmer A., Wallner T., Ringler J., Gerbig F.: H_2-Direct Injection – A Highly Promising Combustion Concept, SAE-Paper 05P-117